Journal of Industrial and Engineering Chemistry xxx (xxxx) xxx

Contents lists available at ScienceDirect

Journal of Industrial and Engineering Chemistry

journal homepage: www.elsevier.com/locate/jiec

The study of *m*-pentadecylphenol on the inhibition of mild steel corrosion in 1 M HCl solution

Emanuel X. Ricky [a,b], Musa Mpelwa [c,1], Xingguang Xu [a,*]

[a] Department of Petroleum Engineering, Faculty of Earth Resources, China University of Geosciences, 388# Lumo Road, Wuhan, Hubei Province 430074, China
[b] Department of Chemistry, College of Natural and Applied Sciences, University of Dar es Salaam, P.O. Box 35061, Dar es Salaam, Tanzania
[c] Department of Science and Information Technology, Faculty of Science and Technology, Teofilo Kisanji University, P.O. Box 1104, Mbeya, Tanzania

ARTICLE INFO

Article history:
Received 29 January 2021
Revised 28 April 2021
Accepted 30 May 2021
Available online xxxx

Keywords:
Corrosion inhibition
Cashew nut shell liquid
m-pentadecylphenol
Mild steel
Adsorption

ABSTRACT

The acidic fluids used in the acidification of oil wells provoke corrosion of metallic materials unenviably. As a consequence, corrosion inhibitors are needed to mitigate or retard the corrosion process. Herein, we report *m*-pentadecylphenol as an eco-friendly corrosion inhibitor in acidic media developed from cashew nut shell liquid (CNSL), which is a low-cost and sustainable source. The inhibitor was evaluated as corrosion inhibitor for mild in 1 M HCl corrosive solution by potentiodynamic polarization (PDP), electrochemical impedance spectroscopy (EIS), weight loss, Fourier transform infrared (FT-IR) spectroscopy, atomic force microscopy (AFM), and energy-dispersive X-ray fluorescence (EDX-RF) spectrometry methods. The results showed that the inhibition efficiency of *m*-pentadecylphenol was at least 95% at an optimal concentration (300 ppm). The inhibition efficiency was found to increase as the inhibitor concentration increments from 100 to 300 ppm. Further studies revealed the inhibition performance of *m*-pentadecylphenol to be marginally reliant on temperature as the temperature rises from 303 to 333 K. At 333 K, the inhibition performance of the inhibitor was still promising (about 85%) when the concentration was 300 ppm. The adsorption studies revealed the spontaneous aptitude of *m*-pentadecylphenol to inhibit corrosion by forming a non-conductive inhibitive layer on the mild steel surface mainly through the chemisorption mechanism. The chemisorption adsorption was satisfactorily described by the Langmuir adsorption isotherm model. Besides, the potentiodynamic polarization measurements revealed *m*-pentadecylphenol to act as an anodic inhibitor. The overall findings revealed that *m*-pentadecylphenol to be an effective corrosion inhibitor in harsh corrosive vicinities with the added advantages of being eco-friendly and relatively cheaper. Thus, it can replace the use of non-green and expensive corrosion inhibitors in the industry.
© 2021 The Korean Society of Industrial and Engineering Chemistry. Published by Elsevier B.V. All rights reserved.

Introduction

Mild steel is one of the most popular alloys of iron with a wide range of industrial applications [1]. It is utilized tremendously for different purposes worldwide due to its high mechanical strength and low cost as compared to carbon steel and stainless steel [1–4]. In the oil and gas industry, mild steel materials are widely used for the construction of oil and gas pipelines, offshore structures, storage tanks, boilers, tubing, borehole, casing, valves, and pumps [5–7]. Apart from their great usefulness, mild steel and its composites are highly susceptible to corrosion when they are exposed to their operating environments [8,9]. Corrosion refers to the degradation of a metal by chemical or electrochemical reaction with its surroundings [10,11]. Metals get corroded when they are exposed to the corrosive vicinities rich in CO_2, H_2S, Cl^-, H^+, SO_4^{2-}, H_2O and dissolved O_2 [12,13].

In the oil and gas industry, corrosion is inevitable due to the use of acids that provoke the deterioration of metal materials [2,3,14]. Acids such as hydrochloric acid and methanoic acid are often used during oil-well acidizing and descaling processes. Oil-well acidizing is implemented during the fracturing process to initiate fractures in the formation that will ensure good fluid communications between the rock formation and the wellbore, thereby increasing the fluid flow into the wellbore [15–17]. In the descaling process, acids are used to dissolve mineral scales which are often formed due to incompatible mixing of waters [18]. Summarily, the corrosion of industrial equipment is a major concern in most

* Corresponding author.
E-mail address: xuxingguang@cug.edu.cn (X. Xu).
[1] ORCID: https://orcid.org/0000-0003-0762-285X.

https://doi.org/10.1016/j.jiec.2021.05.047
1226-086X/© 2021 The Korean Society of Industrial and Engineering Chemistry. Published by Elsevier B.V. All rights reserved.

Please cite this article as: E.X. Ricky, M. Mpelwa and X. Xu, The study of *m*-pentadecylphenol on the inhibition of mild steel corrosion in 1 M HCl solution, Journal of Industrial and Engineering Chemistry, https://doi.org/10.1016/j.jiec.2021.05.047

of the oil and gas industries as it may cause flow assurance problems, declined oil-well productivities, additional production costs, reduced safety, and environmental pollution [19,20]. In this case, corrosion prevention is the cornerstone aspect for profitable petroleum production and the prolonged lifespan of metallic materials used for construction [21].

Generally, corrosion of metallic materials may be mitigated or eradicated by suitable engineering design, metal surface amendments (e.g., electroplating, galvanizing, and coating), electrical control (cathodic and anodic protection), and the application of passive alloys. Other corrosion preventive methods include the modification of the environments (e.g., pH regulation and elimination of corrosive species) and the use of corrosion inhibitors [22,23]. Among several preventive methods, the deployment of corrosion inhibitors is the nascent method for preventing and retarding corrosion in the oil and gas industry which is more versatile, practical, environmentally friendly and cost-effective than other methods [24–26].

The so-called corrosion inhibitors are chemical compounds that when present in the corrosion system at suitable concentrations retard or eradicate the corrosion process, without considerably altering the concentration of any corrosive agent [27]. Corrosion inhibitors often adsorb on the metal surface forming an extremely thin inhibitive layer that prevents direct contact between the metal and corrosive vicinities. In so doing, the corrosion of metallic materials is prevented or retarded at very low inhibitor concentrations [12,28,29]. The compounds comprising of conjugated pi-bonds, aromatic nucleus, and hetero-atoms are well-known to exhibit fabulous corrosion inhibition properties [1,2,6,14]. The existence of these functionalities enhances the adsorption of the inhibitor molecules on the metal surface resulting in the formation of a stable inhibitive layer. Predominantly, organic corrosion inhibitors containing heteroatoms such as nitrogen (N), oxygen (O), and sulfur (S) atoms with lone pair of electrons, and aromatic ring(s) with large alkyl chains in their structures demonstrate excellent corrosion inhibitive behaviors.

Unfortunately, many conventional corrosion inhibitors used to retard or prevent corrosion in corrosive systems are becoming unacceptable due to environmental concerns [30]. For instance, the applications of synthetic corrosion inhibitors such as phosphate, chromate, silicate, and nitrate-containing inhibitors are strictly depressed as they cause environmental and health complications [31–33]. As a consequence, the development of alternatively cheap, readily available, and eco-friendly corrosion inhibitors in the industry is momentously demanded [10,34–36].

Researches have shown that green corrosion inhibitors, which are eco-friendly corrosion inhibitors obtained from low-cost and sustainable natural sources demonstrate little or no environmental concerns as compared with current commercially available corrosion inhibitors [27,30,37,38].

Cashew nutshell (CNS) is a by-product of the cashew industry [39] which is readily available as waste. The shells contain a dark reddish-brown viscous liquid called cashew nut shell liquid (CNSL), mainly composed of anacardic acid, cardanol, cardol and a trace amount of 2-methylcardol [40–42]. CNSL is one of the richest natural sources of phenolic compounds with interesting structural characteristics. Phenolic compounds have molecular structures with high electron density associated with the presence of oxygen heteroatom and aromatic ring with an alkyl group (15-carbon side chain) at *meta*-position [40,42]. Because of the interesting structural properties, the major components of the CNSL are prone to a variety of chemical reactions leading to several important industrial chemicals such as anticorrosive-paints, surfactants, stabilizers, anti-oxidants, detergent, coating, dyes, pigments, epoxy resins, and insecticides [39–41]. Up-to-date CNSL has been recognized as a promising green corrosion inhibitor because of its desirable adsorption properties on metallic surfaces [30,40,43,44], it is projected to demonstrate interesting anticorrosion properties. Philip and his co-workers [44] investigated the anticorrosion properties of CNSL for carbon steel in 3% aqueous NaCl solution saturated with CO_2 at 30 °C and pH of 6 under static conditions using electrochemical measurements. The finds revealed that CNSL was capable of inhibiting corrosion over 92% at an optimal concentration of 300 ppm. Moreover, Philip and his co-workers [25] specifically investigated the anticorrosion properties of amino pentadecylphenols (APPs), semisynthetic compounds derived from CNSL. The results showed that APPs can inhibit the mild steel from corroding in aerated 0.10 M HCl at 303 K to about 98% when an optimal concentration of 600 ppm is applied. Furtado et al., [30] recently developed eco-friendly corrosion inhibitors based on CNSL for acidizing fluids. They developed eight inhibitor formulations by mixing CNSL, the residue obtained after distillation of CNSL, and the cardanol (the main constituent of CNSL). Solvents and acetylenic alcohol were added into the formulations as intensifiers. Interestingly, the formulations demonstrated inhibition efficacies of about 99.47% for API P110 carbon steel in 15% HCl at 298–353 K through both weight loss and electrochemical measurements.

Despite the interesting afore-mentioned discussion on the promising anticorrosion properties ascribed to CNSL, researches on enhancing the corrosion inhibition performance of CNSL is limited. Thus, researches focusing on improving the corrosion inhibition performances of the CNSL or its components present noteworthy determinations toward the development of green corrosion inhibitors. In the current study, cardanol which is the major component of technical CNSL was chemically modified as an effort to enhance the inhibition properties of phenolic compounds derived from CNS. Nonetheless, the study is aimed at developing an eco-friendly corrosion inhibitor from a relatively cheap and readily available biomass by-product, which exhibits high inhibition efficacy in harsh corrosive conditions. The newly designed corrosion inhibitor (*m*-pentadecylphenol) was semi-synthesized via hydrogenation of cardanol derived from CNSL. Structurally, *m*-pentadecylphenol comprises oxygen (O) with lone pair of electrons as a heteroatom and an aromatic ring alkylated with a long alkyl chain. These structural features are decidedly required for better corrosion prevention [45,46]. The designed corrosion inhibitor was systematically studied as a potential corrosion inhibitor for mild steel in 1 M HCl corrosive solution by weight loss and electrochemical measurements.

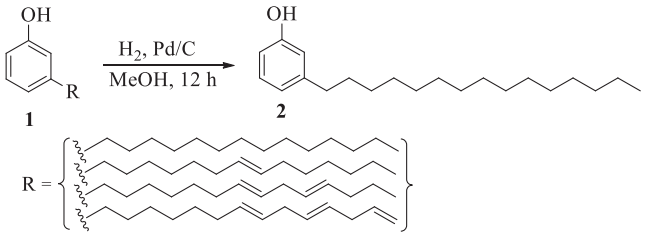
Experimental part

Materials

All chemicals and reagents used in this work were purchased from Sigma Aldrich (South Africa). The solvents and reagents were of analytical grade and they were used as supplied. The chemicals used in this study include methanol (99.8%), ethanol (95%), acetone (99.5%) palladium catalyst (10%) on activated carbon, concentrated HCl (37%) and 3 M KCl (reference electrode filling solution). Other materials used include Whatman filter paper, silicon carbide paper, mild steel coupons and thin-layer chromatography (TLC: 20 × 20 cm, 60G/F254).

Synthesis of m-pentadecylphenol

Cardanol as a starting material for the semi-synthesis of *m*-pentadecylphenol was thermally extracted from CNS as reported elsewhere [47–49]. The extracted cardanol (1) was subsequently hydrogenated to *m*-pentadecylphenol (2) as summarized



Scheme 1. Semi-synthetic method of *m*-pentadecylphenol.

in Scheme 1. The reaction conditions were optimized during hydrogenation to ensure a high purity yield. The *m*-pentadecylphenol obtained was purified and structurally characterized. The per cent yield of the purified *m*-pentadecylphenol was found to be 80% and its melting point was found to range from 323 to 324 K. The FT-IR spectrum of *m*-pentadecylphenol shows absorption band (v/cm^{-1}) at 3359 (O–H), 2915 and 2848 (C–H sp^3 hybridized carbon), 1609 and 1587 (C=C aromatic ring), 1454 and 1314 (CH_2 and CH_3 bending vibrations, respectively), and 1266, 1158, 1113 and 1046 (C–O stretching vibrations) and 785 (*meta*-substituted benzene ring).

Preparation of metal substrates and solutions

Mild steel samples

Mild steel samples were mechanically cut into cylindrical disc coupons with a diameter of 1.1 cm and thickness of 0.2 cm having a surface area of 2.6 cm^2. The surface of the coupons was abraded with a sequence of silicon carbide paper of different grades (320, 800, 2400 and 4000 grit) to obtain a spotless and mirror-like surface. The coupons were then washed with distilled water, degreased with ethanol and acetone, dried with a piece of a soft cloth and stored in a desiccator before they were used for corrosion studies.

Corrosive test and inhibitor solutions

A corrosive test solution of 1 M HCl was prepared with analytical grade 37% HCl and distilled water. A stock inhibitor solution of 1000 ppm was prepared by mixing accurate amounts of *m*-pentadecylphenol prepared and 1 M HCl solution. The tested inhibitor solutions (100–400 ppm) were prepared by mixing accurately measured stock inhibitor solution with the corrosive test solution.

Solubility of m-pentadecylphenol

The solubility of *m*-pentadecylphenol was determined by the conductivity method [50,51]. The electrical conductivities of *m*-pentadecylphenol solutions were measured using a conductivity meter (DDSJ-319L) at 300 K. The solubility of the corrosion inhibitor was graphically deduced by using the electrical conductivity data.

Corrosion studies

In the present study, the corrosion inhibition properties of *m*-pentadecylphenol on mild steel in 1 M HCl solution were studied by using potentiodynamic polarization (PDP), electrochemical impedance spectroscopy (EIS), and weight loss methods. The electrochemical measurements (Open Circuit Potential (OCP), PDP, and EIS measurements) were performed using a Metrohm Autolab Potentiostat (PGSTAT20, Serial no: AUT970464) connected to a three-electrode electrochemical cell. The cylindrical mild steel coupons were used as a working electrode (WE), two stainless steel rods (SS 316) as a counter electrode (CE), and Ag/AgCl electrode filled with 3 M KCl solution as a reference electrode (RE). The electrochemical experiments were performed in a 250 mL capacity double wall Pyrex glass container filled with a corrosive test solution (1 M HCl) in the absence and presence of various concentrations of *m*-pentadecylphenol.

Open circuit potential (OCP) measurements

The values of OCP were measured for the mild steel coupons exposed in 1 M HCl solution before potentiodynamic and electrochemical impedance measurements. The variation of potential with time for the mild steel coupons immersed in 1 M HCl solution in the absence and presence of various concentrations of *m*-pentadecylphenol at zero current and 303 K was recorded by using a potentiostat. The OCP values for the mild steel coupons with respect to Ag/AgCl reference electrode were taken every 30 min for 8 h and after every 1 h from 8 to 13 h.

Potentiodynamic polarization measurements

The potentiodynamic polarization curves were measured by sweeping the electrode potential from −100 mV to +100 mV versus open circuit potential at 1 mV/s scan rate. This scan rate was found appropriate for the corrosion system under this study based on the pilot experiment conducted. All potentiodynamic polarization measurements were done at 303 K without any stirring after 8 h immersion of the working electrode in the test solution. Each experiment was performed three times to obtain a satisfactory reproducibility of the experimental data. From the potentiodynamic polarization curves, various electrochemical parameters were deduced for evaluating the inhibition kinetics and performance of the tested inhibitor. The cathodic (β_c) and anodic (β_a) Tafel slopes, corrosion current densities (i_{corr}) and corrosion potentials (E_{corr}) parameters were obtained through extrapolation of the Tafel lines from the polarization curves at 5 mV to 10 mV from the open circuit potential anodically and cathodically. Both the corrosion rate (*CR*) and the inhibition efficiency (η) were also deduced. The *CR* in millimeter per year (mmy^{-1}) was calculated using Eq. (1) [1]:

$$CR = \frac{i_{corr} \times EW}{A \times \rho \times F} \tag{1}$$

where *EW* is the equivalent weight (g/eq), *A* is the exposed surface area of mild steel (cm^2), ρ is the density of mild steel (g/cm^3), and *F* is the Faraday's constant (C/mol). The inhibition efficiency (η) in per cent (%) was calculated using Eq. (2) [45]:

$$\eta = \left(\frac{CR_o - CR_i}{CR_o}\right) \times 100 \tag{2}$$

where CR_o and CR_i are the values of the corrosion rates of mild steel in the absence and presence of the inhibitor, respectively.

Electrochemical impedance measurements

The electrochemical impedance spectroscopy (EIS) analysis which is a powerful method for detailed corrosion inhibition behaviors of organic inhibitors and their protection mechanisms was carried out in this study. The electrochemical impedance curves were measured using a frequency response analyser (FRA) at a frequency range of 10,000 Hz–0.1 Hz, using AC signals of 10 mV amplitude at the open circuit potential. All EIS measurements were carried out at 303 K without any stirring after 8 h immersion of the working electrode in the test solution. Each experiment was performed three times to obtain a satisfactory reproducibility of the experimental data.

After the EIS measurements, an electrical equivalent circuit (EEC) which consists of solution resistance (R_s), polarization resistance (R_p) and constant phase element (*CPE*/*Q*) has been used to analyze the EIS data through a complex non-linear least-square

curve fitting [52]. Various equivalent circuit parameters includingR_s, R_p, *CPE* and a dimensionless value (n) were obtained after the curve fitting and the readings were taken from the best-fit semicircle with $0.7 \leq n \leq 1$. The obtained values of R_p were used to calculate the inhibition efficiency (η) according to Eq. (3) [53].

$$\eta = \left(\frac{R_p - R_p^o}{R_p}\right) \times 100 \tag{3}$$

where R_p and R_p^o are polarization resistance in the presence and absence of inhibitor, respectively.

In the present study, the *CPE* was introduced instead of a pure double-layer capacitance (C_{dl}) to better fit the experimental data with the proposed equivalent circuit model since the double layer capacitance at the interface does not behave as an ideal capacitor [54]. However, a more reliable equivalent circuit model can be provided by the double-layer capacitance [55]. The values of the C_{dl} were calculated by using Eq. (4) [52,56].

$$C_{dl} = Q\left(R_s^{-1} + R_p^{-1}\right)^{(n-1)/n} \tag{4}$$

Weight loss measurements

The clean-dry mild steel coupons were pre-weighed. The coupons were immersed in 50 mL of 1 M HCl solution with different concentrations of the inhibitor (0–300 ppm) at several temperatures of 303, 313, 323 and 333 K for 24 h. After immersion tests, the specimens were cleaned and reweighed according to the standard method of ASTM G31-72. The immersion tests were triply conducted for each experiment for data reproducibility. The corrosion rate (*CR*) was calculated using Eq. (5) [56].

$$CR = \frac{W.K}{D.A.t} \tag{5}$$

where W is the weight loss (g), K is the constant (8.76×10^4), D is the density of mild steel (g/cm^3), A is the exposed surface area (cm^2), and t is the exposure time (h).

Surface and elemental analyses

Adsorption film analysis

To confirm the formation of protective film on the mild steel due to adsorption of the inhibitor, the specimens were investigated by attenuated total reflection (ATR) spectroscopy after 24 h immersion in 1 M HCl in the absence and presence of 300 ppm of *m*-pentadecylphenol at 303 K. The analyses were carried out by using the Fourier Transform Infra-Red (FT-IR) Spectrometer (Alpha ATR-BRUKER, Gmbh 2011); the scanning range was from 4000 to 400 cm^{-1}.

Surface analysis

The surface morphology and surface roughness parameters of the freshly polished mild steel surface and mild steel surface exposed in 1 M HCl solution in the absence and presence of 300 ppm of the inhibitor were analyzed by using Veeco Instrument, Nanoscope IIIA Atomic Force Microscope (AFM) (AFM, Multi-Sync FE750). The two-dimension (2-D) and three-dimension (3-D) images of the mild steels coupons were taken at a scale of 2 μm × 2 μm. The 2 μm × 2 μm image data of the mild steel coupons were analyzed by using Gwydion and WSxM software's as reported by Ollotu et al. [57].

Elemental analysis

The elemental analyses of mild steel surface exposed in 1 M HCl solution in the absence and the presence of 300 ppm of inhibitor were done by energy-dispersive X-ray fluorescence (EDX-RF 7000) spectrometer.

Results and discussion

Solubility of m-pentadecylphenol

The solubility of corrosion inhibitors is one of the factors that determine their effectiveness [30,58,59]. The inhibitor is anticipated to demonstrate a desirable solubility in the phase system that is targeted for its application [59]. Consequently, the solubility of *m*-pentadecylphenol was evaluated in a 1 M HCl corrosive solution. Fig. 1 displays the plot of electrical conductivity versus inhibitor concentration from which the solubility of the inhibitor was deduced. The solubility of *m*-pentadecylphenol was determined to be 0.49 mM, which is, the maximum concentration that demonstrates an optimal conductivity.

As is shown in Fig. 1, the electrical conductivity initially increased significantly with the increase in the concentration of *m*-pentadecylphenol and thereafter decreased remarkably. The increased and decreased trends observed were attributed to the ability of *m*-pentadecylphenol to exist in deprotonated and protonated forms, respectively. At lower concentrations, *m*-pentadecylphenol ionized (deprotonated) to great extent causing the increased ions concentration in solution thereby triggering the conductivity of the solution. Meanwhile, the ionization of *m*-pentadecylphenol decreased as the inhibitor concentration increases beyond its solubility. The non-ionized molecules were protonated causing a reduced concentration of hydrogen ions in the solution thereby decreasing the electrical conductivity of the solution as the inhibitor concentration increases. Generally, *m*-pentadecylphenol was sparingly soluble in 1 M HCl solution as supported by its electrical conductivity measurement results. In the present, the solubility of *m*-pentadecylphenol was not enhanced using organic solvents. Furthermore, previous studies have reported that the corrosion inhibitors with high solubility cannot provide long-term active corrosion protection of the coated alloy because of the very fast release of the inhibitor from the coating [60]. Thus, the corrosion inhibitive compounds with low solubility might be preferable candidates for incorporation into the surface of the coated alloy [60].

Open circuit potential (OCP)

The OCP measurement is one of the vital tasks in determining the required immersion time for the electrochemical system to attain a relatively steady-state condition before performing any electrochemical measurements [61]. In the present study, the values of OCP as a function of time were recorded for the mild steel coupons immersed in 1 M HCl solution in the absence and presence of various concentrations of *m*-pentadecylphenol, and the results obtained are shown in Fig. 2.

The results show that for all the corrosive test solutions the OCP values become more negative with increasing immersion time, indicating the dissolution of the mild steel surface by the aggressive chloride ions attack [62]. The results in Fig. 2 depict a significant decrease in OCP values for all the corrosive test solutions up to 2 h immersion time and a gradual decrease in OCP values from 2 h to almost 8 h. Eventually, the OCP reached stable values after 8 h immersion time, reflecting the completion of the mild steel surface dissolution by the corrosive agents or formation of the passive layer of inhibitor or corrosion products over the mild steel surface which protects the mild steel surface and stop its dissolution. In the present study, all electrochemical measurements were performed after 8 h immersion of mild steel in 1 M HCl solution in

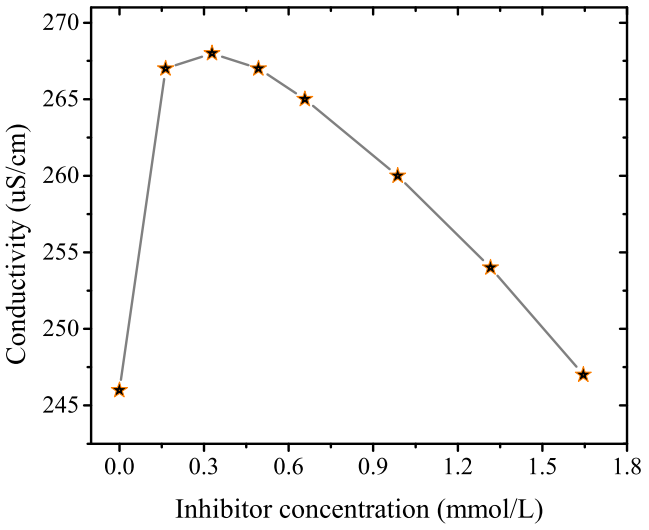


Fig. 1. Conductivity as a function of *m*-pentadecylphenol concentration.

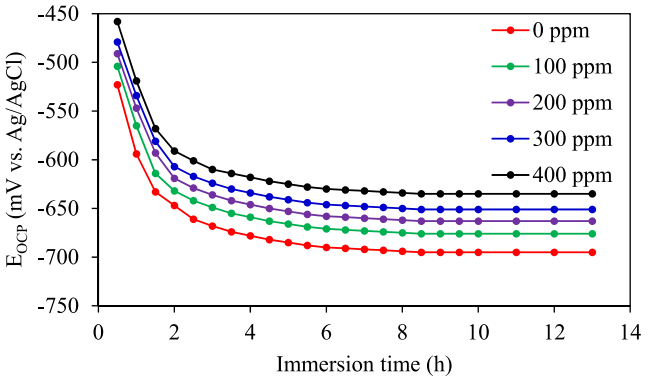


Fig. 2. Variation of OCP with time for mild steel immersed in a 1 M HCl solution in the absence and presence of various concentrations of *m*-pentadecylphenol at 303 K.

the absence and presence of various concentrations of *m*-pentadecylphenol. The results also show that the increase in the concentration of *m*-pentadecylphenol shifted both the absolute and the steady-state OCP values to a more positive direction due to the increased adsorption of the inhibitor molecules on the mild steel surface. This positive shift of the OCP in the presence of inhibitor indicates that the inhibitor has influenced the anodic reaction of mild steel corrosion as reported elsewhere [62,63].

Potentiodynamic polarization

The potentiodynamic polarization measurements were carried out to evaluate the effect of the addition of inhibitor on the anodic and cathodic polarization curves for mild steel in 1 M HCl solution without and with various concentrations of m-pentadecylphenol at 303 K. The potentiodynamic polarization curves for mild steel in 1 M HCl without and with various concentrations of *m*-pentadecylphenol at 303 K are shown in Fig. 3. The electrochemical parameters such as corrosion potential (E_{corr}), corrosion current density (i_{corr}), anodic Tafel slope (βa) and cathodic Tafel slope (βc) have been obtained via extrapolation of the linear parts of the anodic and cathodic lines. The corrosion rate (*CR*) and inhibition efficiency (η) was calculated using Eqs. (1) and (2), respectively. The results for these electrochemical parameters are given in Table 1. From Fig. 3, it is clear that the anodic curves shift to lower values of corrosion current densities more than the cathodic curves with

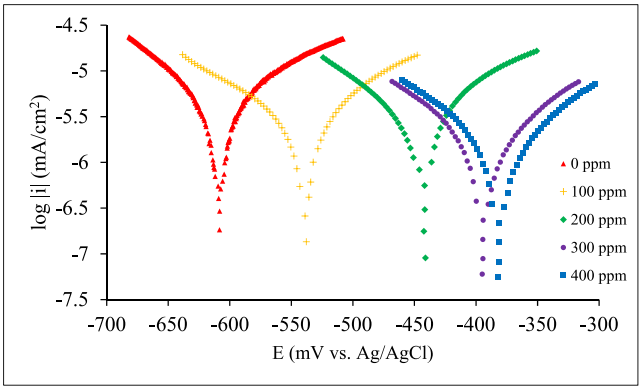


Fig. 3. Potentiodynamic polarization curves for the corrosion of mild steel in 1 M HCl solution in the absence and presence of inhibitor at 303 K.

the increasing concentration of the inhibitor (*m*-pentadecylphenol), suggesting that the anodic dissolution of the mild steel was inhibited [64]. Table 1 clearly shows that the anodic Tafel slope (βa) and cathodic Tafel slope (βc) vary slightly independent of the inhibitor concentration. This observation indicates that there is no major change in the corrosion mechanism of the mild steel in 1 M HCl solution in the absence and presence of the studied inhibitor. Thus, the studied corrosion inhibitor is believed to act by simply blocking the active sites on the mild steel surface and decrease the surface area for the corrosion process [65].

The results in Table 1 showed that both corrosion current density (i_{corr}) and corrosion rate (*CR*) decreases as the inhibition efficiency (η) increases significantly with the increase in inhibitor concentration below its optimal concentration. This kind of behaviors could be attributed to a strong interaction between *m*-pentadecylphenol molecules and the mild steel surface, suggesting the adsorption of inhibitor molecules on the mild steel surface forming a protective layer on the mild steel surface [55]. The decrease in i_{corr} and *CR* with the increasing inhibitor concentration confirmed that the addition of *m*-pentadecylphenol has reduced the dissolution of mild steel in 1 M HCl solution. The least *CR* (0.052 mmy^{-1}) and i_{corr} (4.510 $\mu A/cm^2$), and the maximum η (95%) were observed at optimal inhibitor concentration (300 ppm), above which insubstantial changes were observed.

The results in Fig. 3 also revealed that in the presence of *m*-pentadecylphenol inhibitor, the corrosion potential (E_{corr}) shifted toward a more positive direction. Table 1 clearly shows that the values of E_{corr} become more positive with the increasing concentration of the inhibitor. Previous literature reported that, if the displacement in E_{corr} is more than 85 mV with respect to E_{corr} of the blank, the inhibitor can be classified as cathodic or anodic type, and if the displacement in E_{corr} is less than 85 mV the corrosion inhibitor may be regarded as a mixed type [1,45,52]. In the present study, the maximum shift in E_{corr} was 226 mV toward positive direction with respect to the $E_{corr}$of the blank. This implies that the studied corrosion inhibitor is an anodic inhibitor, predominantly affecting the anodic reaction on retarding the corrosion process [65]. In summary, the PDP results demonstrated the ability of *m*-pentadecylphenol to inhibit the corrosion of mild steel even under severe corrosive environments. Its inhibition ability is quite better and comparable to the most studied corrosion inhibitors [1,17,45,46,52].

Electrochemical impedance spectroscopy

The accumulation of solution species on the mild steel surface during the corrosion process results in the formation of an electric

Table 1
Potentiodynamic polarization parameters for the corrosion of mild steel in 1 M HCl solution at 303 K.

C_{inh} (ppm)	β_a(mV dec^{-1})	$-\beta_c$(mV dec^{-1})	$-E_{corr}$(mV vs. Ag/AgCl)	i_{corr}(μA cm^{-2})	CR (mmy^{-1})	η(%)
0	15 ± 0.101	16 ± 0.149	608 ± 0.431	90.203 ± 0.084	1.046	0
100	13 ± 0.089	14 ± 0.127	538 ± 0.263	19.845 ± 0.062	0.230	78.0
200	14 ± 0.050	17 ± 0.118	441 ± 0.086	7.213 ± 0.032	0.084	91.9
300	15 ± 0.035	17 ± 0.121	395 ± 0.165	4.510 ± 0.057	0.052	95.0
400	13 ± 0.071	15 ± 0.127	382 ± 0.048	4.228 ± 0.014	0.049	95.3

double layer with capacitance and resistance properties to charge transfer [55]. The electric double layer formed can affect the mechanism and rate of electron transfer between the cathodic and anodic sites on the mild steel surface. The EIS is one of the best methods that provide reliable information on the dielectric properties of the metal-solution interface, the adsorption mechanism of inhibitors on the mild steel surface, and the kinetics of the electrochemical reactions [55]. Therefore, the corrosion behavior of the mild steel in 1 M HCl solution in the absence and presence of different concentrations of *m*-pentadecylphenol at 303 K was studied using EIS. The Nyquist plot with an equivalent circuit model and Bode plot for the mild steel in 1 M HCl solution in the absence and presence of different concentrations of *m*-pentadecylphenol at 303 K are shown in Figs. 4 and 5, respectively. The electrochemical parameters such asR_s, R_p, Q, and n obtained from the Nyquist curves fitting in the equivalent circuit model shown in Fig. 4 are presented in Table 2. The calculated values of η and C_{dl} using Eqs. (3) and (4), respectively are also given in Table 2.

Fig. 4 shows that the Nyquist plots are characterized by depressed semicircles with one capacitive loop. This is attributed to the roughness and inhomogeneity of the mild steel surface due to corrosion [1,52]. The diameters of the semicircles increased substantially with an increase in the concentrations of *m*-pentadecylphenol to the optimal concentration, above which the semicircles diameters increased negligibly. This phenomenon is attributed to the ability of *m*-pentadecylphenol molecules to retard the dissolution of the mild steel surface in the corrosive solutions presumably by forming the protective layer on the mild steel surface that enhances the corrosion resistance. The imperfections of semicircles decreased with the increment in the inhibitor concentration because of the improved smoothness of the mild steel surface. The roughness and inhomogeneity of the mild steel surface decreased as the inhibitor concentration increments due to reduced corrosion of the mild steel surface. This can be affirmed with the values of n in Table 2 which increases with the increasing concentration of the inhibitor. The values of n provide information on the roughness of the mild steel surface, a small value of n is indicative of a rough surface [66].

Furthermore, the Bode plots (Fig. 5) show a single maximum phase angle at around intermediate frequency (2.4 Hz). The maximum phase angle becomes wider with the increasing concentration of the inhibitor, implying the formation of the protective layer on the mild steel surface. The higher values of phase angle for the inhibited solution than the uninhibited solution reflect the corrosion inhibitive action of the inhibitor used [54]. Fig. 5 also shows that the value of impedance increases with the increasing concentration of the studied inhibitor. This indicates that the corrosion of mild steel surface is reduced in presence of the studied inhibitor. Fig. 4 shows the strong agreement between the experimental data and fitted lines implying the accuracy of the EIS measurements.

The results shown in Table 2 reveal that the values of R_s, R_p, n and $\eta(\%)$ increased significantly with the increase in inhibitor concentration. This is due to the formation of the protective layer of inhibitor as *m*-pentadecylphenol molecules adsorb on the mild steel surface and decrease the surface area for the corrosion process [54]. The protective layer formed on the mild steel surface creates a barrier against the release of electrons from the metal surface, thereby increasing corrosion resistance and improve inhibition efficiency. Furthermore, it is evident from Table 2 that the values of C_{dl} and Q decrease with the increasing concentration of the inhibitor. This implies the decrease in the dielectric constant through replacement of the pre-adsorbed corrosive species on the mild surface with the inhibitor molecules [55]. This process increases the thickness of the electrical double layer and reduces the surface area of the mild steel exposed to corrosive agents [45,46].

Summarily, the EIS studies revealed a desirable ability of *m*-pentadecylphenol to prevent corrosion of metal in acidic media. Its optimal inhibition under experimental conditions is 94% which is in good order with the results obtained from PDP analyses. Besides, the low values of the goodness of fit (χ^2) in Table 2 show that the fitted data agree well with the experimental data, suggesting the validity of the proposed equivalent circuit.

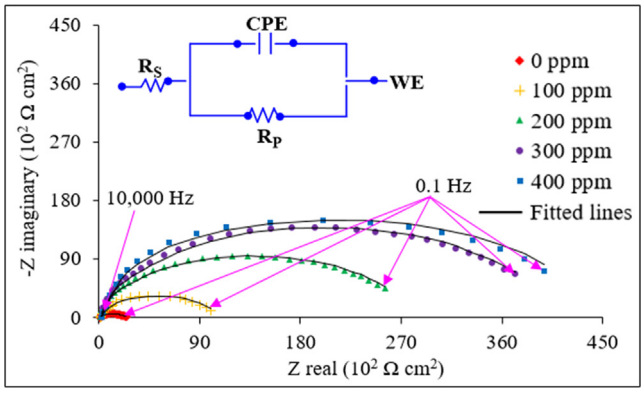


Fig. 4. Nyquist plot with an equivalent circuit model for the mild steel in 1 M HCl solution in the absence and presence of different concentrations of the inhibitor at 303 K.

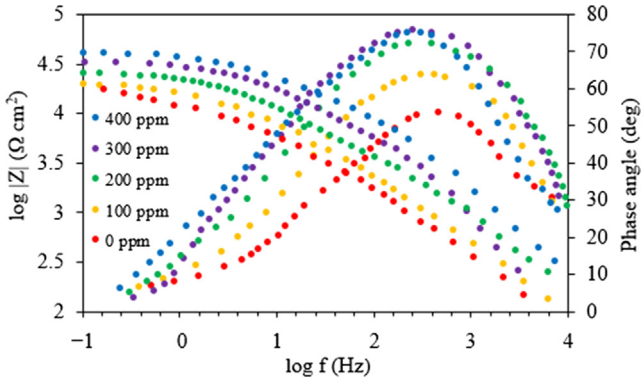


Fig. 5. Bode plots of mild steel in 1 M HCl solution in the absence and presence of different concentrations of the inhibitor at 303 K.

Table 2
Electrochemical impedance parameters for the corrosion of mild steel in 1 M HCl solution at 303 K.

C_{inh} (ppm)	$R_s(\Omega.cm^2)$	$R_p(\Omega.cm^2)$	Q ($\mu F.cm^{-2}$)	n	χ^2 10^{-3}	$C_{dl}(\mu F.cm^{-2})$	$\eta(\%)$
0	16.02 ± 0.109	2356.12 ± 0.050	568.19 ± 0.028	0.70095 ± 0.045	1.16	1850	–
100	50.23 ± 0.059	9996.84 ± 0.007	162.74 ± 0.047	0.70101 ± 0.003	0.72	863	76.4
200	150.62 ± 0.045	25618.30 ± 0.015	107.06 ± 0.002	0.74038 ± 0.002	0.32	622	90.8
300	164.67 ± 0.044	30379.50 ± 0.042	59.75 ± 0.007	0.74439 ± 0.005	0.49	344	92.2
400	182.83 ± 0.005	40106.40 ± 0.072	57.40 ± 0.036	0.76307 ± 0.058	0.86	289	94.1

Adsorption isotherms

The adsorption mechanism of the inhibitor molecules on the metal surface can be evaluated through adsorption isotherms. The adsorption isotherms are very important in understanding the adsorption mechanism of the inhibitor molecules on the active sites of the metal surface [1]. In this study, the adsorption mechanism of *m*-pentadecylphenol on the mild steel surface was investigated through different adsorption isotherms including Frumkin, Freundlich, Temkin, and Langmuir adsorption isotherms. Among these adsorption isotherms, the Langmuir adsorption isotherm described satisfactorily the adsorption mechanism of the investigated inhibitor with a correlation coefficient (R^2) value of about a unit (Fig. 6a and b). The Langmuir adsorption isotherms were studied using the linear form of the Langmuir adsorption isotherm (Eq. (6)) [45].

$$\frac{C_{inh}}{\theta} = \frac{1}{K_{ads}} + C_{inh} \tag{6}$$

where θ is the surface coverage, C_{inh} is the inhibitor concentration, and K_{ads} is the adsorption/desorption equilibrium constant. The values of K_{ads} were deduced from the plots of C_{inh}/θ versus C_{inh} (Fig. 6 (a, b and c)) by equating $\frac{C_{inh}}{\theta}$ intercept with $\frac{1}{K_{ads}}$. The change in Gibb's free energy of adsorption (ΔG°_{ads}) that describes the interaction between inhibitor species and the metal surface substrate was calculated using Eq. (7) [1].

$$\Delta G^{\circ}_{ads} = -RTln(55.5K_{ads}) \tag{7}$$

where R is the molar gas constant (8.314J.mol^{-1}.K^{-1}), 55.5 is the molar concentration of water (mol.L^{-1}), and T is the absolute temperature (K). The calculated values of K_{ads} and ΔG°_{ads} are given in Table 3 and were found to be in good agreement for all methods. Ostensibly, the ΔG°_{ads} values suggest the inhibitor molecules mainly adsorbed on the mild steel surface through chemisorption [9,23]. The chemisorption was believed to arise due to the release of unshared electron pairs mainly π-electrons of the aromatic ring of inhibitor into vacant d-orbital of the iron species assuming dative bonding [23]. The more negative values of ΔG°_{ads} affirmed the spontaneous chemisorption process resulting in the formation of a stable protective layer. Thus, *m*-pentadecylphenol inhibitor can effectively protect the metal surface from corrosion by blocking the active sites of the metal that are susceptible to corrosion by forming a non-conductive and inhibitive layer through chemical adsorption. Besides, the values of ΔG°_{ads} were fairly found to be the same as the temperature increases (Table 3). The fairly constant in ΔG°_{ads} values were associated with the steady change in the adsorption mechanism as the temperature increases. The adsorption mechanism of *m*-pentadecylphenol onto the mild steel substrate remained intact owing to the increase in temperature. This infers to the ability of the inhibitor to offer fairly the same inhibition efficiencies at different temperatures. Additionally, the decrease in K_{ads} with the increase in temperature suggests desorption of inhibitor from the steel surface. The inhibition efficiency slightly decremented as the temperature increases due to the desorption of the inhibitor.

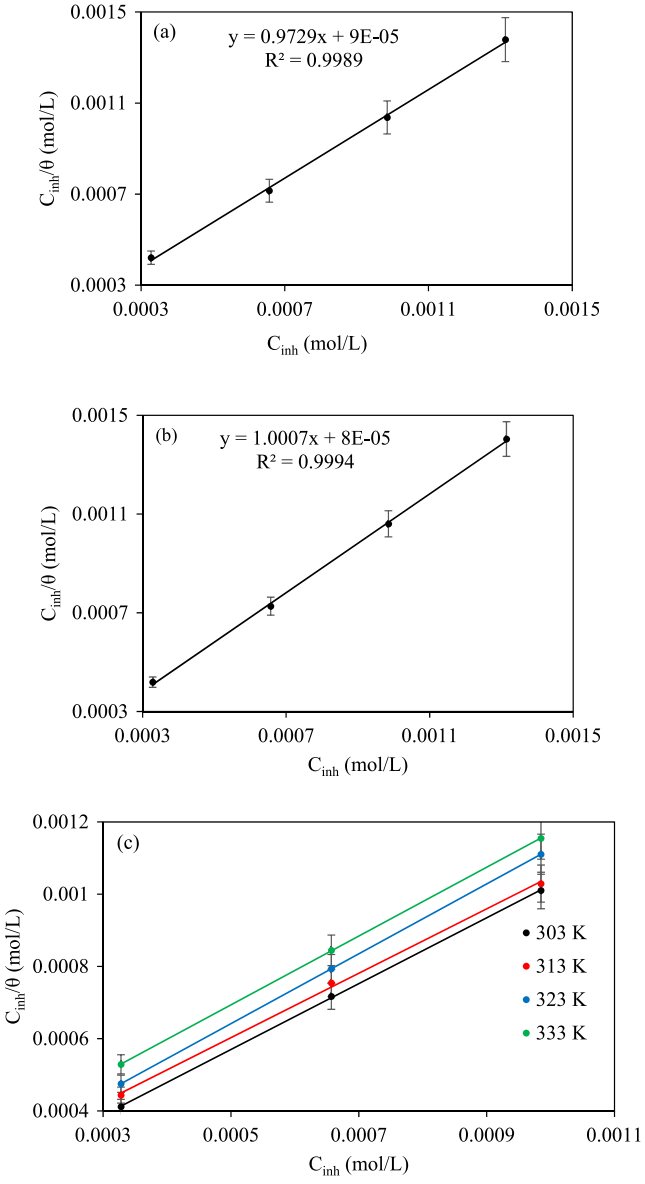


Fig. 6. Langmuir adsorption isotherms of *m*-pentadecylphenol for the corrosion of mild steel in 1 M HCl solution: (a) PDP at 303 K, (b) EIS at 303 K, and (c) weight loss method at 303, 313, 323, and 333 K.

Temperature and activation parameters

Temperature affects significantly both the corrosion rate and the adsorption efficacies of the corrosion inhibitors [52]. To investigate the influence of temperature on the inhibition efficacy of the

Table 3
Adsorption parameters obtained from PDP, EIS and weight loss method for the Langmuir adsorption isotherms of mild steel in 1 M HCl solution.

Method	Temperature (K)	R^2	Intercept (10^{-3}mol.L^{-1})	K_{ads}(10^3L.mol^{-1})	ΔG°_{ads}(kJ.mol^{-1})
PDP	303	0.9989	0.09	11.11	−33.592
EIS	303	0.9994	0.08	12.50	−33.888
Weight loss	303	0.9999	0.10	10.00	−33.326
	313	0.9999	0.10	10.00	−34.425
	323	1	0.12	8.70	−35.152
	333	1	0.13	7.69	−35.898

studied inhibitor, the weight loss method was used at various temperatures. Generally, the inhibition efficacy of *m*-pentadecylphenol was still promising (about 85%) at high temperatures despite the marginally decremented trend observed as temperature increases (Fig. 7). The decrease in inhibition efficiency is due to the increased corrosion rate as temperature rises (Table 4). Also, *m*-pentadecylphenol molecules presumably desorbed from the mild steel surface as the temperature increases. This provoked the deterioration of mild steel due to the exposed unprotected metal sites.

Furthermore, the activation parameters including apparent activation energy (E_a), apparent enthalpy of activation (ΔH^*) and apparent entropy of activation (ΔS^*) that describe fastidiously the dependence of inhibitor adsorption on temperature were deduced. The E_a for the corrosion process was determined using the Arrhenius Equation that describes the dependence of the corrosion rate on temperature, Eq. (8) [1].

$$lnCR = -\frac{E_a}{R}\left(\frac{1}{T}\right) + lnA \tag{8}$$

where CR is the corrosion rate (mmy^{-1}), E_a is the apparent activation energy (J.mol^{-1}), R is the molar gas constant (8.314J.mol^{-1}.K^{-1}), T is the absolute temperature (K), and A is the pre-exponential factor. The E_a was deduced from the slope of the Arrhenius plot ($E_a = -R.slope$). The values of apparent enthalpy (ΔH^*) and apparent entropy (ΔS^*) of activation were calculated from the transition-state Equation (Eq. (9)) [1,67].

$$ln\left(\frac{CR}{T}\right) = \left[ln\left(\frac{R}{N.h}\right) + \Delta S^*\right] - \Delta H^*\left(\frac{1}{T}\right) \tag{9}$$

where h is the Planck's constant (6.626×10^{-34}J.s), N is the Avogadro's number (6.023×10^{23}mol^{-1}), and other symbols carry the usual meanings. The ΔH^* was deduced from the slope of the transition-state plot i.e., $\Delta H^* = -R.slope$, whereas the ΔS^* was calculated from the intercept i.e. $\Delta S^* = ln\left(\frac{R}{Nh}\right)$ − intercept. The plots of $lnCR$ versus $1/T$ and $ln(CR/T)$ versus $1/T$ both demonstrated satisfactorily linearity with correlation coefficient (R^2) values of nearly a unit (Figs. 8 and 9).

The values of E_a, ΔH^*, and ΔS^* are presented in Table 5. From the results, the inhibited systems have higher values of E_a than the uninhibited system. The higher values of E_a affirm the ability of the inhibitor molecules to adsorbed on the mild steel surface creating a protective barrier. The protective barrier generated bolstered the energy barrier for the corrosion process to occur, thereby retarding the corrosion rate. The E_a values were found to increase as the concentration of inhibitor increases to the optimal concentration. This is associated with the increase in the formation of a non-conductive and inhibitive film as the concentration of inhibitor increases, thereby increased the energy barrier for the corrosion process progressively. It is important to note that the rise of E_a in the presence of inhibitor defined the possible chemisorption mechanisms of the *m*-pentadecylphenol on the mild steel surface [6]. The chemisorption is more emphasized by ΔH^* (112.21 kJ.mol^{-1}) greater than 100 kJ.mol^{-1} [64]. The chemisorption is believed to arise due to the release of electron pairs from inhibitor molecule into vacant d-orbital of the iron species assuming dative bonding as described previously. Moreover, ΔH^* was revealed to be positive defining the possible endothermic adsorption of inhibitor on the steel substrate [23]. The ΔH^* values were high suggesting the chemisorption adsorption of the inhibitor on the steel surface. The adsorption increased as the concentration of inhibitor increases following the increased ΔH^* values. The increased adsorption efficiency as the inhibitor concentration increases is emphasized with the observed trend for ΔS^* that increased with the increase in concentration [23]. Nonetheless, ΔS^* (positive value) endorses the disordered arrangement of the species during the rate-determining step [1]. This may be associated with the dissociation of some intermediate corrosion products such as desorption of adsorbed chloride ions or water molecules from the mild steel surface to allow the adsorption of the inhibitor molecules on the mild steel surface.

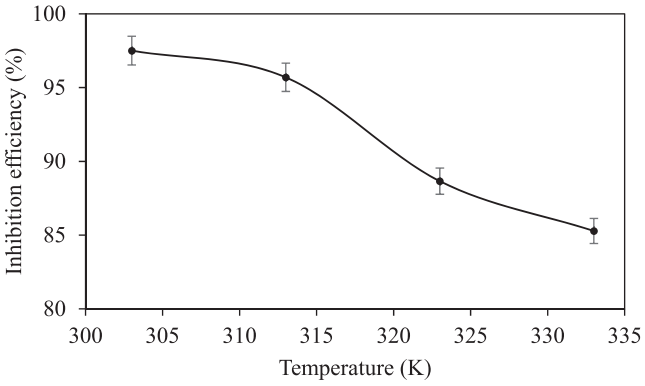


Fig. 7. Effect of temperature on inhibition efficacy of 300 ppm of *m*-pentadecylphenol in 1 M HCl solution.

Surface and elemental analyses

Adsorption film analysis

The ATR-FTIR spectra were used to examine the formation of a protective adsorption layer on the surface of the mild steel which was immersed in 1 M HCl solution containing 300 ppm *m*-pentadecylphenol for 24 h. The ATR-FTIR spectra of pure *m*-pentadecylphenol and the protective layer formed on the mild steel surface are shown in Fig. 10 for comparison. Ostensibly, the spectra observed for *m*-pentadecylphenol and the surface of the protected mild steel are characteristically comparable. Both of them displayed the existence of C=C, C–O, OH, CH_2, and CH_3 groups which are the main groups in *m*-pentadecylphenol. This phenomenon gives a clue that the inhibitor molecules were adsorbed onto the surface of the mild steel to form a film that played a role in resisting a metal from corroding. Predominantly, the comparison of the ATR-FTIR spectra of the pure *m*-pentadecylphenol and the deposited protective layer on the mild steel coupon immersed in 1 M HCl containing 300 ppm inhibitor reveals some noticeable

Table 4
Experimental parameters obtained from weight loss measurements in 1 M HCl in the absence and presence of various concentrations of *m*-pentadecylphenol at different temperatures.

Test solution	Temperature (K)	Weight Loss (mg)	*CR* (mmy^{-1})	η (%)
Blank	303	56.10 ± 0.004	10.1061	–
	313	237.0 ± 0.015	42.6940	–
	323	380.0 ± 0.031	68.4546	–
	333	549.7 ± 0.022	98.3687	–
100 ppm	303	11.40 ± 0.007	2.0399	79.7
	313	61.80 ± 0.012	11.0586	73.9
	323	117.9 ± 0.021	21.0973	69.0
	333	208.8 ± 0.016	37.3632	62.0
200 ppm	303	4.700 ± 0.001	0.8410	91.6
	313	30.60 ± 0.013	5.4756	87.1
	323	65.30 ± 0.017	11.6850	82.8
	333	122.3 ± 0.038	21.8847	77.8
300 ppm	303	1.400 ± 0.001	0.2522	97.5
	313	10.20 ± 0.004	1.8375	95.7
	323	43.10 ± 0.006	7.7642	88.7
	333	80.90 ± 0.011	14.4770	85.3

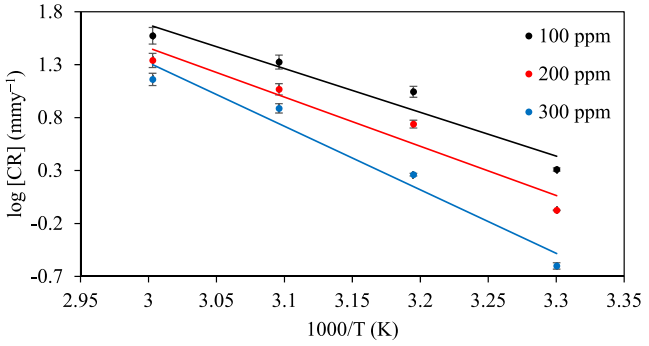


Fig. 8. Arrhenius plots of log *CR* versus 1000/T for mild steel corrosion in 1 M HCl solution in the presence of various concentrations of *m*-pentadecylphenol.

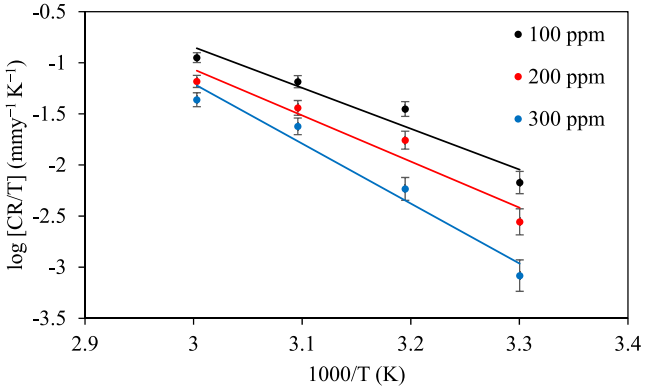


Fig. 9. Transition state plot for the corrosion rate of mild steel in 1 M HCl in the presence of various concentrations of *m*-pentadecylphenol at 303, 313 and 323 K.

Table 5
Activation parameter obtained from weight loss measurements for mild steel in 1 M HCl solution in the presence of various concentrations of *m*-pentadecylphenol.

System	E_a (kJ.mol^{-1})	ΔH^* (kJ.mol^{-1})	ΔS^* (J.mol^{-1}.K^{-1})
Blank	61.94	59.30	−27.87
100	79.16	76.52	15.79
200	89.00	86.36	41.12
300	114.85	112.21	116.00

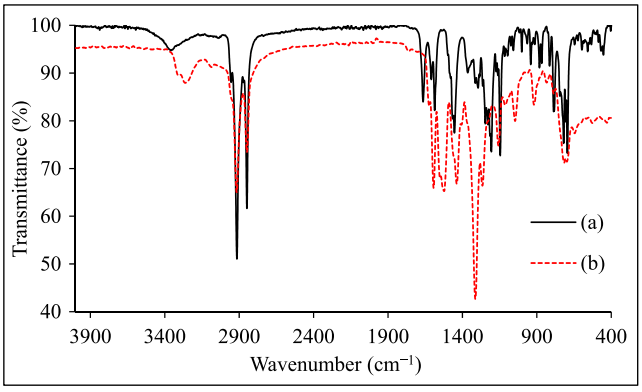


Fig. 10. The ATR-FTIR spectra of *m*-pentadecylphenol (a) and a protective film (b) formed on the mild steel surface in 1 M HCl solution.

variations in chemical shifts. The variations are as follow: a shift from 3359.93 cm^{-1} to 3263.01 cm^{-1} due to O–H stretching [68]; the bands associated with C–O stretching shifted from 1294.48, 1017.41 cm^{-1} to 1266.03, 1046.54 cm^{-1} [68]; the vibration bands due to C=C for aromatic ring shifted from 1608.98, 1586.53 cm^{-1} to 1593.97, 1523.24 cm^{-1} [68].

The observed displacements in some functional groups including C=C and O–H, toward lower wavenumbers, are attributed to the chemical interaction between inhibitor molecules and the mild steel substrates during the formation of a protective layer. The OH and C=C nucleophilic groups chemically interact with mild steel substrates via dative bonding and/or electrostatic interactions [1,45]. During chemical interactions, the nucleophilic groups presumably donated their electron pairs into the vacant d-orbitals of the Fe^{2+} (dative bonding) forming or participated in electronic attraction with the mild steel substrates (electrostatic attraction) Fe^{2+}-inhibitor complex. Consequently, the protective layer was formed onto the mild steel surfaces to which the functional groups that participated in chemical interactions exhibited lower absorption frequencies.

AFM and EDX analyses

The AFM images and surface roughness parameters for the freshly polished mild steel surface and mild steel surfaces in 1 M HCl solution in the absence and presence of 300 ppm of *m*-pentadecylphenol after 24 h at 303 K are depicted in Fig. 11(a–c) and Table 6, respectively. In general, both the AFM images and sur-

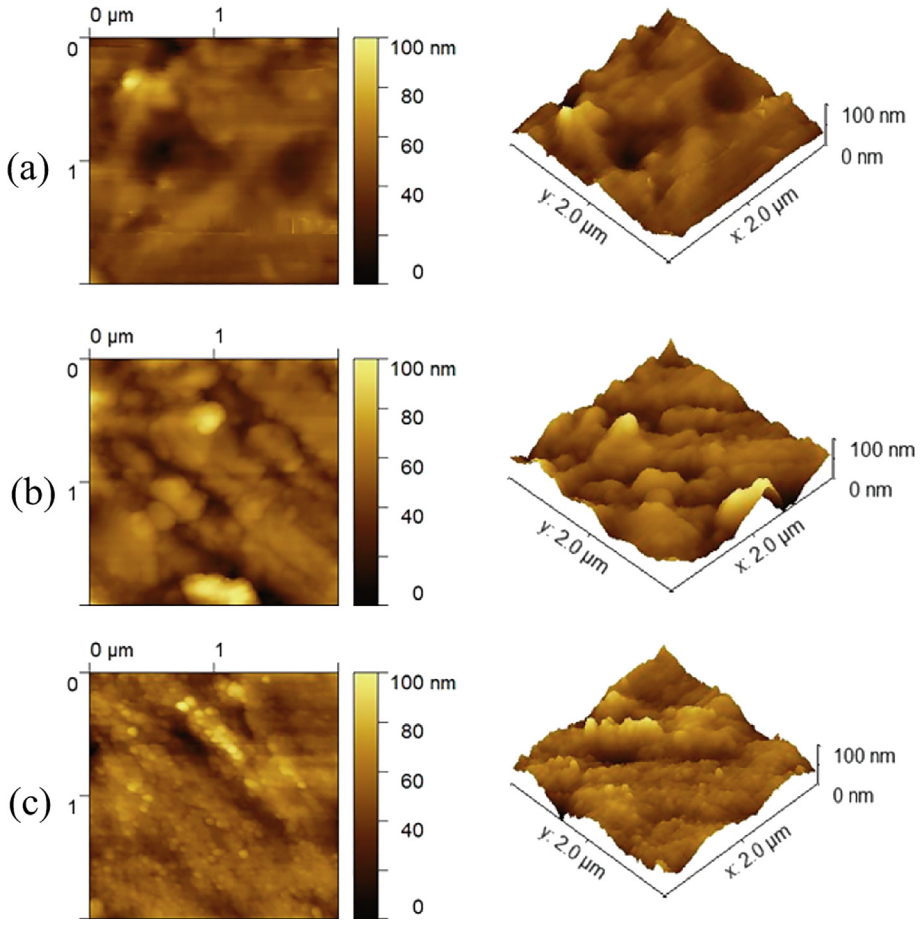


Fig. 11. The AFM images: (a) polished mild steel, (b) mild steel in 1 M HCl solution in the absence of inhibitor, and (c) mild steel in 1 M HCl in the presence of 300 ppm of *m*-pentadecylphenol.

Table 6
Surface roughness parameters for the polished mild steel, mild steel in 1 M HCl solution in the absence inhibitor and mild steel in 1 M HCl in the presence of 300 ppm of *m*-pentadecylphenol.

Sample ID	Polished mild steel	Mild steel in 1 M HCl without inhibitor	Mild steel in 1 M HCl with inhibitor
RMS roughness (nm)	6.755	37.041	9.592
Average roughness (nm)	5.440	28.566	6.962
Average height (nm)	31.207	121.080	31.698

face roughness parameters (grain size/average height, average roughness and root mean square (RMS) roughness) show a smoother surface in the presence of an inhibitor comparable with that of the freshly polished mild steel surface. On the contrary, the surface of mild steel is rougher with pits due to extreme corrosion in acidic media in the absence of the corrosion inhibitor as supported by the surface roughness parameters of the mild steel in 1 M HCl without inhibitor and AFM images (Fig. 11b). This concludes that the addition of *m*-pentadecylphenol inhibitor reduced the corrosion rate of the mild steel due to the formation of a protective layer of inhibitor. The formation of a stable protective layer of inhibitor on the mild steel surface suggests that *m*-pentadecylphenol can significantly protect the surface of the mild steel from corrosion in acidic media.

Nevertheless, EDX was also employed to determine the elemental composition of the mild steel surface in the absence and presence of the 300 ppm of *m*-pentadecylphenol inhibitor in 1 M HCl solution after 24 h at 303 K. The EDX results are shown in Table 7 and Fig. 12. It can be noted from Table 7 and Fig. 12 that the elemental composition of Fe is higher for the mild steel immersed 1 M HCl solution in the presence of 300 ppm of *m*-pentadecylphenol inhibitor than in the absence of the inhibitor. The higher Fe content in the inhibited mild steel is an indication for the reduced corrosion rate attributing to the adsorption of the inhibitor molecules on the mild steel surface forming a stable inhibitive layer. Besides, in the absence of an inhibitor, the metal surface contained a substantial amount of chloride contrarily with the presence of 300 ppm of *m*-pentadecylphenol.

Proposed inhibition mechanism

Electrochemical degradation of metallic materials occurs spontaneously resembling a galvanic cell process. The anodic and cathodic reactions occur during the corrosion process. A metal (M) is oxidized by corrosive agents such as Cl^-, H^+, H_2O, and O_2 causing the loss of electrons (e^-) to its surroundings. The lost electrons reduce other species such as H_2O on the metal surface. In the absence of an inhibitor, the oxidized species (M^{n+}) and reduced species (OH^-) react together to form metal hydroxides [$M(OH)_n$] which may react further with oxygen and water to form hydrated metal oxides (Fig. 13a). In the presence of an inhibitor, the corrosion process is interrupted to avoid further degradation of the metal. The corrosion inhibitor (*m*-pentadecylphenol) preferentially bind to the metallic substrates through the lone pair electrons of the O atom and π-electrons of the aromatic ring. These pair electrons are donated to the vacant d-orbitals of the metal atom, creat-

Table 7
Elemental composition of mild steel surface from EDX analysis.

	Elemental composition (%)							
	Fe	Mn	Al	Cu	Ca	Sn	Sr	Cl
Blank	86.77	0.43	7.17	0.07	0.04	0.06	0.01	5.46
300 ppm Inhibitor	90.74	0.44	8.67	0.07	0.08	–	0.01	–

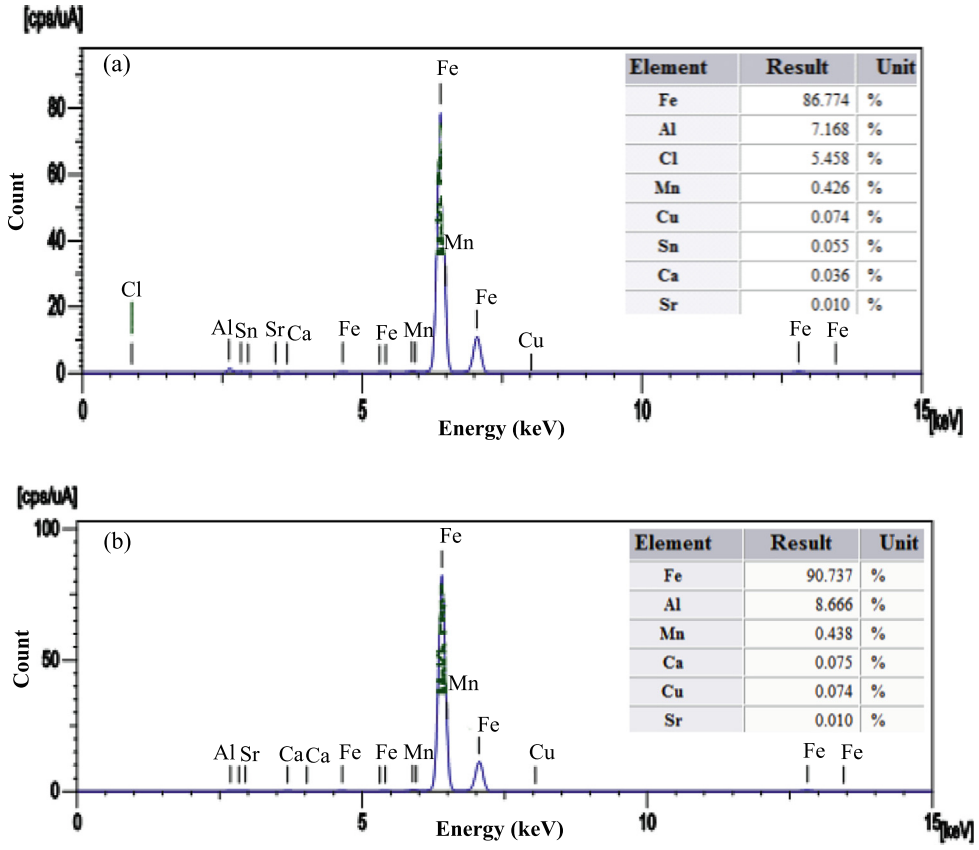


Fig. 12. EDX spectra of mild steel immersed in 1 M HCl solution in the absence of *m*-pentadecylphenol (a) and the presence of 300 ppm of *m*-pentadecylphenol (b).

ing electrostatic interactions with the positively charged metal surface. In so doing, a non-conductive protective layer is formed on the metal surface that acts as a barrier to corrosive agents (Fig. 13 b). Thus, the corrosion process is stopped as the energy needed to destroy the protective layer is higher.

Conclusion

The present study investigated the corrosion inhibition performance of *m*-pentadecylphenol on mild steel in 1 M HCl solution. The following conclusions were drawn:

(1) The inhibition efficiency of *m*-pentadecylphenol increased with the increase in the concentration of the inhibitor from 100 to 300 ppm. The maximum inhibition efficiency reached about 95% (electrochemical methods) and 98% (weight loss method) in the presence of 300 ppm of inhibitor at 303 K.
(2) The inhibition efficiency of *m*-pentadecylphenol was found to depend on the inhibitor concentration and temperature.
(3) The adsorption of *m*-pentadecylphenol inhibitor onto the mild steel surface obeys the Langmuir adsorption isotherm model mainly through the chemisorption mechanism.
(4) The polarization resistance (*Rp*) and double-layer capacitance (C_{dl}) values were found to increase and decrease, respectively with the increase in inhibitor concentration due to the increased thickness of the protective layer on the mild steel surface.
(5) The addition of optimum concentration of the inhibitor significantly reduces the corrosion damage of mild steel through the formation of a non-conductive protective layer. Besides, *m*-pentadecylphenol acts as an anodic inhibitor on retarding the corrosion of the mild steel.

The overall findings from several methods proved *m*-pentadecylphenol as an effective corrosion inhibitor for mild steel in acidic media. The inhibitor may be used to prevent corrosion with added merits of being eco-friendly and readily available.

Declaration of Competing Interest

The authors declare that they have no known competing financial interests or personal relationships that could have appeared to influence the work reported in this paper.

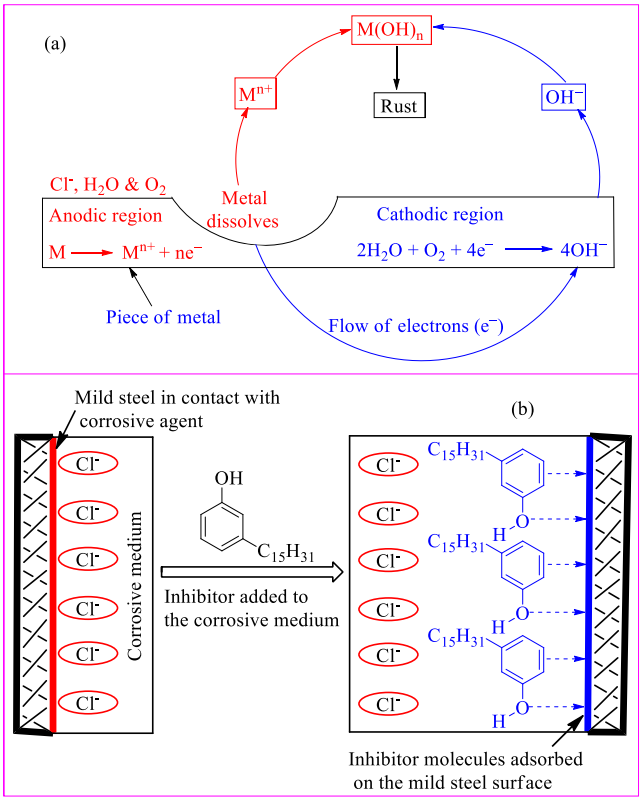


Fig. 13. Schematic representation of a corrosion process and proposed adsorption mechanism of *m*-pentadecylphenol on mild steel surface in 1 M HCl solution.

Acknowledgements

The authors are grateful to the International Science Programme (ISP–Sweden), Dr. Nuru R Mlyuka, and Mr. E. R. Ollotu from the Department of Physics, University of Dar es Salaam, Tanzania, for assisting in the AFM analyses.

References

[1] T. Peme, L.O. Olasunkanmi, I. Bahadur, A.S. Adekunle, M.M. Kabanda, E.E. Ebenso, Molecules 20 (2015) 16004–16029, https://doi.org/10.3390/molecules200916004.
[2] Y. Sangeetha, S. Meenakshi, C.S. Sundaram, Carbohydr. Polym. 150 (2016) 13–20, https://doi.org/10.1016/j.carbpol.2016.05.002.
[3] P. Singh, E.E. Ebenso, L.O. Olasunkanmi, I.B. Obot, M.A. Quraishi, J. Phys. Chem. C. (2016), https://doi.org/10.1021/acs.jpcc.5b11901.
[4] R.T. Loto, O. Olowoyo, South African J. Chem. Eng. 26 (2018) 35–41, https://doi.org/10.1016/j.sajce.2018.09.002.
[5] F. Ackson, Corros. Sci. 86 (2014) 17–41, https://doi.org/10.1016/j.corsci.2014.04.044.
[6] S. Manimegalai, P. Manjula, J. Mater. Environ. Sci. 6 (2015) 1629–1637, https://doi.org/http://www.jmaterenvironsci.com.
[7] G. Karthik, M. Sundaravadivelu, Egypt. J. Pet. 25 (2016) 183–191, https://doi.org/10.1016/j.ejpe.2015.04.003.
[8] O.E. Osokogwu, Int. J. Sci. Technol. Res. 1 (2012) 19–23, https://doi.org/www.ijstr.org.
[9] A. Espinoza-va, M. Romero-romo, J. Aldana-gonza, J. Uruchurtu-chavarin, M. Palomar-pardave, Arab. J. Chem. (2015) 1–10, https://doi.org/10.1016/j.arabjc.2015.08.033.
[10] Z. Tang, Curr. Opin. Solid State Mater. Sci. (2019) 1–16, https://doi.org/10.1016/j.cossms.2019.06.003.
[11] R.W. Revie, Corrosion and an Introduction to Corrosion Science and Engineering, 4th ed., John Wiley & Sons Inc., 2008.
[12] L.T. Popoola, A.S. Grema, G.K. Latinwo, B. Gutti, Int. J. Ind. Chem. (2013) 1.
[13] R.A. Anaee, M.H. Alzuhairi, H.A. Abdullah, Asian J. Eng. Technol. 02 (2014) 2321–2462, https://doi.org/www.ajouronline.com.
[14] E. Telli, G. Karda, B. Yaz, J. Mol. Liq. 218 (2016) 384–392, https://doi.org/10.1016/j.molliq.2016.02.087.
[15] Z. Yahui, T. Shanfa, W. Jiaxin, M. Mpelwa, P. Mingzheng, Z. Tianyuan, Arab. J. Sci. Eng. 44 (2019), https://doi.org/10.1007/s13369-018-3552-0.
[16] M. Mpelwa, Y. Zheng, S. Tang, M. Pu, L. Jin, Chem. Eng. Commun. (2019) 1–9, https://doi.org/10.1080/00986445.2019.1660650.
[17] M. Mpelwa, S. Tang, L. Jin, R. Hu, C. Wang, Y. Hu, J. Pet. Sci. Eng. 186 (2020), https://doi.org/10.1016/j.petrol.2019.106799.
[18] M. Mpelwa, S.-F. Tang, Pet. Sci. (2019) 1–20, https://doi.org/10.1007/s12182-019-0299-5.
[19] J. Buchweishaija, Tanz. J. Sci. 35 (2008) 77–92.
[20] M.H. Hussin, M.J. Kassim, J. Phys. Sci. 21 (2010) 1–13.
[21] S. Pathapalya, M.H. Ananda, R.V. Beema, J. Chil. Chem. Soc. 4 (2012) 1364–1371.
[22] E.X. Ricky, E.H.J. Lugwisha, J.Y.N. Philip, Tanz. J. Sci. 47 (2021) 112–122.
[23] H. Wei, B. Heidarshenas, L. Zhou, G. Hussain, Q. Li, K. Ken, Mater. Today Sustain. 10 (2020), https://doi.org/10.1016/j.mtsust.2020.100044.
[24] N.O. Eddy, J. Adv. Res. 6 (2015) 203–217, https://doi.org/10.1016/j.jare.2014.01.004.
[25] J. Yoeza, N. Philip, J. Buchweshaija, A. Mwakalesi, Mater. Sci. Appl. 7 (2016) 396–402.
[26] Y. Yetri, N. Jamarun, Int. Conf. Biol. Chem. Environ. Sci. (2014) 15–19, https://doi.org/10.15242/IICBE.C614002.
[27] C. Monticelli, Corrosion inhibitors, in: Encycl. Interfacial Chem. Surf. Sci. Electrochem., Elsevier, 2018, pp. 164–171, https://doi.org/10.1016/B978-0-12-409547-2.13443-2.
[28] P.K. Bagavathy, S. Muthu Saravana, Ganesan, J. Chem. Pharm. Res. 7 (2015) 830–839, https://doi.org/www.jocpr.com..
[29] P. Hu, D. Ph, Z. Wu, J. Wang, Y. Huang, Q. Liu, S. Zhou, Chin. Acad. Sci. (2019), https://doi.org/10.1016/j.gee.2019.11.003.
[30] L.B. Furtado, R.C. Nascimento, P.R. Seidl, M.J.O.C. Guimarães, L.M. Costa, J.C. Rocha, J.A.C.P. Ponciano, J. Mol. Liq. 284 (2019) 393–404, https://doi.org/10.1016/j.molliq.2019.02.083.
[31] M.A. Amin, S.S.A. El-rehim, R.S. Bayoumi, Electrochim. Acta 52 (2007) 3588–3600, https://doi.org/10.1016/j.electacta.2006.10.019.
[32] M. Ramezanzadeh, G. Bahlakeh, B. Ramezanzadeh, J. Mol. Liq. 290 (2019), https://doi.org/10.1016/j.molliq.2019.111212.
[33] S.A. Umoren, M.M. Solomon, I.B. Obot, R.K. Suleiman, J. Ind. Eng. Chem. 76 (2019) 91–115, https://doi.org/10.1016/j.jiec.2019.03.057.
[34] K. Shalabi, Y.M. Abdallah, H.M. Hassan, A.S. Fouda, Int. J. Electrochem. Sci. 9 (2014) 1468–1487, https://doi.org/www.electrochemsci.org.
[35] N. Kumpawat, A. Chaturvedi, R.K. Upadhyay, Open J. Met. 2012 (2012) 68–73, https://doi.org/10.4236/ojmetal.2012.23010.
[36] V. Sribharathy, S. Rajendran, P. Rengan, R. Nagalakshmi, Eur Chem. Bull. (2013) 471–476, https://doi.org/10.17628/ECB.2013.2.471.
[37] V. Vorobyova, M. Skiba, O. Chygyrynets, Pigment Resin Technol. 48 (2019) 137–147, https://doi.org/10.1108/PRT-03-2018-0025.
[38] A.E.S. Fouda, A.A. Nazeer, A.Y. El-khateeb, M. Fakih, J. Korean Chem. Soc. 58 (2014), https://doi.org/10.5012/jkcs.2014.58.4.359.
[39] Y. Shi, P.C.J. Kamer, D.J. Cole-hamilton, Green Chem. 21 (2019) 1043–1053, https://doi.org/10.1039/c8gc03823f.
[40] D. Lomonaco, G. Mele, S.E. Mazzetto, Cashew nutshell liquid (CNSL): from an agro-industrial waste to a sustainable alternative to petrochemical resources, in: Cashew Nut Shell Liq. A Goldf. Funct. Mater., Springer International Publishing AG, 2017, pp. 19–38, https://doi.org/10.1007/978-3-319-47455-7.
[41] R.N. Patel, S. Bandyopadhyay, A. Ganesh, Bioresour. Technol. 97 (2006) 847–853, https://doi.org/10.1016/j.biortech.2005.04.009.
[42] S.E. Mazzetto, D. Lomonaco, G. Mele, Quim. Nova. 32 (2009) 732–741, https://doi.org/10.1590/s0100-40422009000300017.
[43] J. Mgaya, G.B. Shombe, S.C. Masikane, S. Mlowe, E.B. Mubofu, N. Revaprasadu, Green Chem. 21 (2019) 1186–1201, https://doi.org/10.1039/c8gc02972e.
[44] J. Philip, J. Buchweishaija, L. Mkayula, Tanzania J. Sci. 27 (2001), https://doi.org/10.4314/tjs.v27i1.18332.
[45] E. Berdimurodov, A. Kholikov, K. Akbarov, G. Xu, A.M. Abdullah, M. Hosseini, Arab. J. Chem. 13 (2020) 7504–7523, https://doi.org/10.1016/j.arabjc.2020.08.025.
[46] M. Faiz, A. Zahari, K. Awang, H. Hussin, RSC Adv. 10 (2020) 6547–6562, https://doi.org/10.1039/c9ra05654h.
[47] C.N. Subbarao, K.K.M. Prasad, V.S.R. Prasad, Pharma Res. J. 06 (2011) 21–41.
[48] T. Tedja, M.A. Nur, I. Sailah, Indones. J. Agric. 2 (2009) 11–20.
[49] T. Himabindu, V. Raguram, S.T. Kumar, Int. J. Inst. Pharm. Life Sci. 5 (2015) 293–308.
[50] M.M. Alam, S. Mahbub, M.M. Hosen, D. Kumar, M.A. Hoque, Chem. Pap. (2021) 1–12, https://doi.org/10.1007/s11696-021-01568-0.
[51] W. Binana-Limbele, R. Zana, Colloid Polym. Sci. 267 (1989) 440–447, https://doi.org/10.1007/BF01410190.
[52] H.M. Elabbasy, H.S. Gadow, J. Mol. Liq. 321 (2021), https://doi.org/10.1016/j.molliq.2020.114918.
[53] A. Berrissoul, A. Ouarhach, F. Benhiba, A. Romane, A. Zarrouk, A. Guenbour, B. Dikici, A. Dafali, J. Mol. Liq. (2020), https://doi.org/10.1016/j.molliq.2020.113493.
[54] M. Yadav, S. Kumar, N. Kumari, I. Bahadur, E.E. Ebenso, Int. J. Electrochem. Sci. 10 (2015) 602–624.
[55] A. Farhadian, A. Rahim, N. Safaei, A. Shaabani, M. Abdouss, A. Alavi, Corros. Sci. (2020), https://doi.org/10.1016/j.corsci.2020.108871.
[56] C.M. Fernandes, L.X. Alvarez, N.E. dos Santos, A.C.M. Barrios, E.A. Ponzio, Corros. Sci. (2019), https://doi.org/10.1016/j.corsci.2019.01.019.
[57] E.R. Ollotu, J.S. Nyarige, N.R. Mlyuka, M.E. Samiji, M. Diale, J. Mater. Sci. Mater. Electron. 31 (2020) 16406–16413, https://doi.org/10.1007/s10854-020-04192-y.

[58] G. Palanisamy, Corrosion inhibitors, in: Corros. Inhib., IntechOpen, 2019, https://doi.org/10.5772/intechopen.80542.
[59] R.C. Woollam, S.J. Merrett, Why water soluble corrosion inhibitors should be the preferred choice for continuous applications, in: Proc. - SPE Annu. West. Reg. Meet., Publ by Society of Petroleum Engineers (SPE), 1994, pp. 205–214, https://doi.org/10.2118/27869-ms.
[60] M.G.S. Ferreira, M.L. Zheludkevich, J. Tedim, K.A. Yasakau, Self-healing nanocoatings for corrosion control, in: Corros. Prot. Control Using Nanomater., Woodhead Publishing Limited, 2012, pp. 213–263, https://doi.org/10.1533/9780857095800.2.213.
[61] M.P. Asfia, M. Rezaei, G. Bahlakeh, M. Rezaei, G. Bahlakeh, J. Mol. Liq. (2020). https://doi.org/org/10.1016/j.molliq.2020.113679.
[62] E.M. Sherif, Int. J. Electrochem. Sci. 6 (2011) 3077–3092.
[63] A.A. Al-amiery, A.A.H. Kadhum, A.H.M. Alobaidy, A.B. Mohamad, P.S. Hoon, Materials (Basel) 7 (2014) 662–672, https://doi.org/10.3390/ma7020662.
[64] L.C. Murulana, M. Kabanda, E.E. Ebenso, RSC Adv. 5 (2015) 28743–28761, https://doi.org/10.1039/C4RA11414K.
[65] M. Yadav, D. Sharma, S. Kumar, Korean J. Chem. Eng. 32 (2015) 993–1000, https://doi.org/10.1007/s11814-014-0275-0.
[66] N.A. Odewunmi, M.M. Solomon, S.A. Umoren, S.A. Ali, ACS Omega 5 (2020) 27057–27071, https://doi.org/10.1021/acsomega.0c02345.
[67] M.P. Chakravarthy, K.N. Mohana, ISRN Corros. 2014 (2014) 1–13, https://doi.org/10.1155/2014/687276.
[68] F.J. Warren, M.J. Gidley, B.M. Flanagan, Carbohydr. Polym. 139 (2016) 35–42, https://doi.org/10.1016/J.CARBPOL.2015.11.066.